

We are IntechOpen, the world's leading publisher of Open Access books Built by scientists, for scientists

6,900

Open access books available

186,000

International authors and editors

200M

Downloads

Our authors are among the

154

Countries delivered to

TOP 1%

most cited scientists

12.2%

Contributors from top 500 universities



WEB OF SCIENCE™

Selection of our books indexed in the Book Citation Index
in Web of Science™ Core Collection (BKCI)

Interested in publishing with us?
Contact book.department@intechopen.com

Numbers displayed above are based on latest data collected.
For more information visit www.intechopen.com



Luminescence Properties of AlN Ceramics and Its Potential Application for Solid State Dosimetry

Laima Trinkler and Baiba Berzina

*Institute of Solid State Physics, University of Latvia
Latvia*

1. Introduction

Aluminum nitride (AlN) is a wide band material ($E_g = 6.2$ eV) with a wurtzite structure. It has already found practical application in microelectronics as substrate, insulator and packaging material due to combination of the uppermost qualities, such as high thermal conductivity, good dielectric properties and thermal expansion coefficient comparable with that of silicon. There are different modifications of the material used for application and investigation purposes: single crystal, powder, nanostructures, thin films and so on. AlN ceramics is one of them, it is easy to produce and to handle, thereat in the form of ceramics AlN maintains the main properties of the material.

The objective of the study is investigation of luminescence properties of AlN ceramics including elucidation of luminescence centers and mechanisms as well as estimation of potential application of the material in the field of solid state dosimetry. This chapter is based on our papers devoted to luminescent and dosimetric properties of AlN ceramics published in 1998-2009 and quite recent measurements performed at low temperatures.

2. Experimental details

2.1 Samples of AlN ceramics

Samples of high-density AlN ceramics were obtained in Institute of Inorganic Chemistry, Riga Technical University, Latvia (Palcevskis et al., 1997; 1999). AlN powder with specific surface area in the range 20-40 m²/g and Y₂O₃ powder (30 m²/g), both produced by plasma synthesis, were used for production of ceramics. Directly after synthesis AlN powders were kept in organic solvent. AlN and Y₂O₃ powders (2-9 wt.%) were mixed in organic media. Then powder mixtures were dried and pressed in cylinders (12 mm in diameter) at 200 MPa. After burning out organic components in vacuum at 500 °C cylinders were embedded into alumina crucibles and placed in a tungsten resistance furnace. The sintering was carried out in nitrogen atmosphere (0.12 MPa) at temperature 1600-1800 °C during 300-900 min. The produced polycrystalline ceramic cylinders were sliced into 1 mm thick tablets, suitable for optical measurements.

Sintered samples were characterized by the producers as follows (Palcevskis et al., 1999). Size of polycrystalline grains is around 4 μm. Depending on sintering conditions

(temperature and time) density varies from 3.2 to 3.4 g/cm³ and thermal conductivity – from 80 to 260 W/mK. AlN grains constitute more than 90% of the volume of the sintered samples; the rest volume belongs to secondary phases: Y₄Al₂O₉, AlYO₃ and Y₃Al₅O₁₂.

Though nominally pure, AlN always contains oxygen impurity as a natural dopant, which substitutes nitrogen in regular lattice sites and forms oxygen-related defects of various types. The total oxygen content in the studied AlN ceramic samples determined by the neutral activation analysis is from 0.1 to 0.7 wt.%. Alongside with oxygen impurity aluminum vacancies are generating for maintenance of charge balance. Besides there are detected other uncontrolled impurities of small concentration (< 1000 ppb) such as Fe, Cr, Ni and Zr. The further spectral measurements have proved the presence of Mn impurity, too. Oxygen and other impurities contribute to luminescence properties of the material.

In some of experiments we used AlN ceramics samples subjected to oxygen ion implantation. This procedure was done in Taiwan National University with doses 10¹⁴ and 10¹⁵ ion/cm².

2.2 Methods of photoluminescence, thermoluminescence and optically stimulated luminescence

Luminescence properties of AlN ceramics were studied using methods of photoluminescence (PL), thermoluminescence (TL) and optically stimulated luminescence (OSL). Photoluminescence is luminescence of material revealed under irradiation with ultraviolet (UV) or visible light. We have used such characteristics of PL as emission spectra obtained under irradiation with a fixed wavelength from UV region and excitation spectra – dependence of luminescence intensity at a fixed emission wavelength upon the varied wavelength of excitation light.

Irradiation of wide band gap materials with UV light and ionizing radiation results not only in immediate response in the form of luminescence but also in ionization – transfer of previously bound charge carriers (electrons and holes) into the conduction band. After relaxation charge carriers can be trapped on trapping centers. Trapping levels remain occupied until supply of additional stimulation energy in the form of heat or light (visible or infrared) releases charge carriers, which can participate in further retrapping or recombination processes with light emission. Such light emission is called TL or OSL depending on type of stimulation energy supplied.

Optically stimulated luminescence is characterized with OSL emission spectra – dependence of emission intensity versus emission wavelength at fixed irradiation wavelength (energy) and dose, OSL excitation spectra – dependence of emission intensity of irradiation wavelength or energy at fixed emission and stimulation wavelength and OSL stimulation spectra – dependence of emission intensity on wavelength of stimulation light at fixed emission and irradiation wavelength. TL is characterized with TL glow curves – dependence of TL emission intensity on heating temperature, TL emission spectra – dependence of emission intensity versus emission wavelength at fixed irradiation wavelength (energy) and dose, TL excitation spectra – dependence of emission intensity of irradiation wavelength or energy at fixed emission wavelength.

2.3 Equipment

Experiments on PL and OSL as well as some TL experiments in the 0-300 °C temperature range were carried out in Institute of Solid State Physics, University of Latvia, Latvia, using an experimental setup for spectroscopic measurements. The setup was equipped with a

deuterium lamp LDD-400 as a source of UV light and a grating monochromator MDR-2 (LOMO) in the excitation channel. The luminescence signal was analyzed either with a prism monochromator SPM-2 (Carl Zeiss Jena) and detected with photo multiplier tubes H7468-03, H7468-20 (Hamamatsu) and FEU-100 (earlier experiments), or with a grating monochromator SR-303i-B (Shamrock) equipped with a CCD camera DV420-BU2. For low temperature measurements samples were inserted into a closed cycle helium refrigerator (Janis) providing stable temperatures in the 8-325 K range. TL measurements were done using a small home-made oven with linear heating up to 300 °C, used as a sample holder in the experimental setup for spectral measurements.

Beta, gamma, X-ray and UV light induced TL and partly OSL measurements were fulfilled in Riso National Laboratory, Denmark, using the available equipment: Riso model TL/OSL readers with linear planchet heating and Alnor Dosacus TLD reader, operating with hot nitrogen heating. For most of irradiations a $^{90}\text{Y}/^{90}\text{Sr}$ beta source build in the Riso TL reader and a ^{60}Co standard gamma calibration facility were used. UV irradiation was performed with a metal halide lamp Sol-2 (K.Honley GmbH), which simulates a solar spectrum at ground level from 300 nm upwards.

Some of TL measurements were done in University of Nice-Sophia Antipolis, LPES-CRESA, France, using a home-made TL reader with linear heating and an optical multichannel analyzer (Princeton Instruments). UV irradiation was carried out with a deuterium lamp (50W) with attached interference filters.

3. Photoluminescence properties of AlN ceramics

Luminescence spectra of AlN were studied using different excitation types; however, excitation with UV light, producing photoluminescence, appeared to be the most informative. PL emission of AlN ceramics was observed in the 300-1100 nm region, which is spectral area of luminescence of defect centers. It contains several emission bands, and for each of them excitation spectrum was measured. Excitation spectra were measured beginning from the fundamental absorption edge (in other words band-to-band transition area) at 200 nm and up to 600 nm. The luminescence region of exciton emission (below 250 nm) is not available with the equipment used and will not be discussed here.

The general view of PL emission spectrum could be illustrated by our recent results on PL measurements of AlN ceramics fulfilled in the 8-300 K temperature range. The following emission bands can be distinguished in the PL spectra at 300 K in Fig.1, a.: a broad UV-blue band in the 300-500 nm region, a narrower band at 600 nm and minor bands at 700 nm and 1000 nm. At low temperature the composition of PL spectrum remains the same, except for emergence of an additional minor band at 500 nm, while relative intensity of emission bands under different excitation wavelengths changes, see Fig.1, b. Contribution of individual bands varies from sample to sample and depends on composition and sintering conditions of ceramics. Let us discuss properties and origin of individual bands.

3.1 Oxygen-related emission

The main attention should be devoted to the broad complex UV-blue band. It is composed of two subbands – those at 400 and 480 nm each of them having its own excitation spectrum. As it is seen from Fig.2. taken from (Berzina et al., 2009), 400 nm emission band has excitation band at 240-250 nm, while 480 nm emission band has excitation band centered at 280-290 nm; both of them are excited also in the fundamental absorption edge at 200-220 nm.

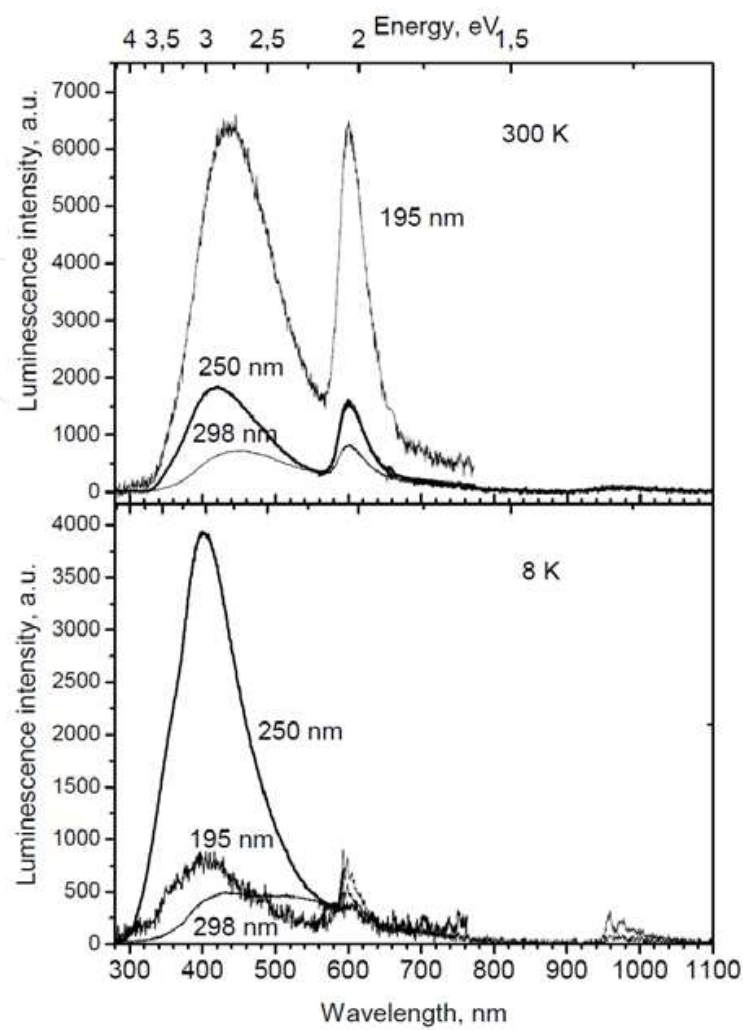


Fig. 1. PL spectra of AlN ceramics at 300 and 8 K, excitation wavelengths shown on the graph

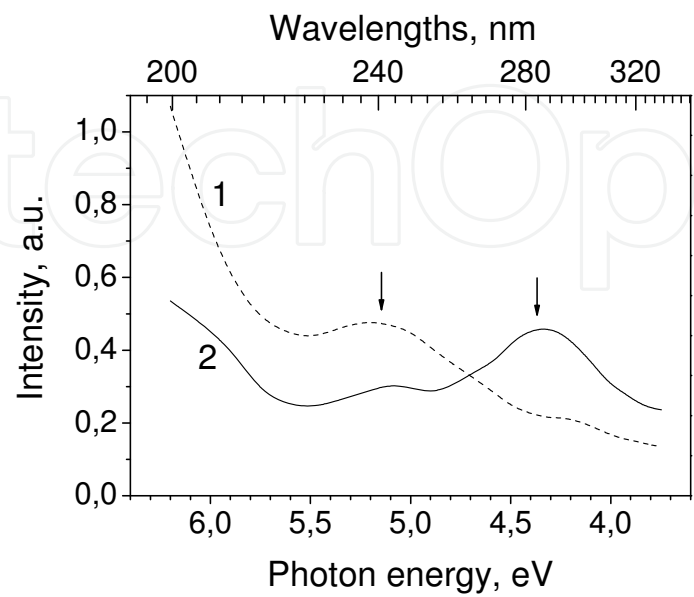


Fig. 2. Excitation spectra of 400 nm (1) and 480 nm (2) emission bands of AlN ceramics at 300 K

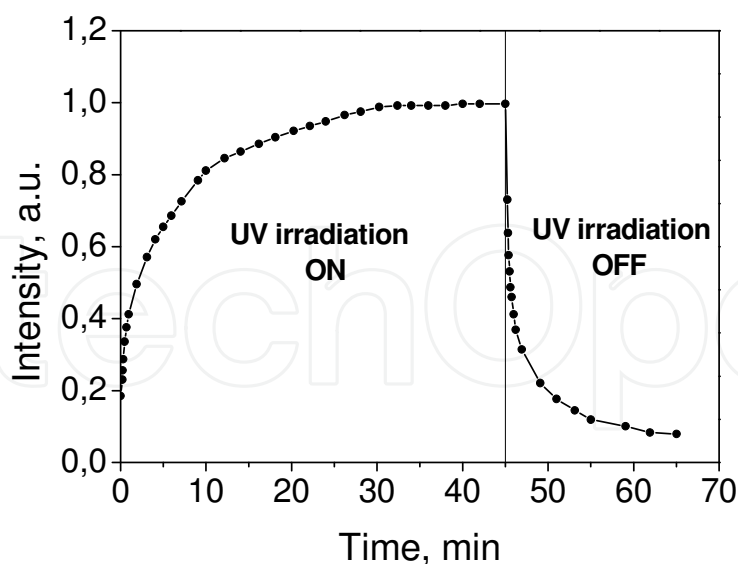


Fig. 3. Time dependence of intensity of the UV-blue emission at start and stop of UV irradiation at 300 K

It was observed in (Berzina et al., 2001) that intensity of the UV-blue emission band depends upon duration of the continuous UV irradiation. As seen from Fig.3, at the beginning of the UV irradiation with 245 nm it is low, and then gradually increases until reaching saturation level after approximately 30 min. After ceasing of UV irradiation the gradually decreasing afterglow emission is observed for several minutes. In the same time position of the maximum of emission band shifts to the longer wavelengths.

Many publications are devoted to elucidating the origin of luminescence centers responsible for the UV-blue band. In (Slack, 1973; Youngman & Harris, 1990 and Harris et al., 1990) it was shown that this band is connected with emission of oxygen-related defects. Later our works (Trinkler et al, 1998, 2001a, 2003, 2005, 2007a, 2007b) have shown that this band is revealed also in TL and OSL emission spectra. Presence of the emission band in PL, TL and OSL as well as afterglow emission and time characteristics of its intensity speak in favor in its recombination character. The nature of the 400 nm subband was determined by the EPR and ENDOR studies (Schweizer et al, 2000) as recombination luminescence of two defect centers: a donor - (O_N-V_{Al}) - a complex defect center formed by an oxygen ion substituting for nitrogen ion O_N in a regular site and a neighboring aluminum vacancy V_{Al} and an acceptor - another closely situated oxygen ion O_N .

The luminescence mechanism responsible for the 400 nm emission band in AlN ceramics, was formulated in papers (Berzina et al., 2002, 2009). The corresponding energy band diagram is shown in Fig. 5. According to it the ($V_{Al}-O_N$) center forms its energy level within the band gap above the valence band (level 5). Irradiation of AlN with 245 nm light from the own absorption band ($h\nu_{def}$) results in its excitation (level 6). The excited state is situated close to the bottom of the conduction band resulting in ionization of the ($V_{Al}-O_N$) center and an electron transfer into the conduction band. An electron from the conduction band can be captured by one of numerous electron traps (levels from 7 up to 11). One of them is an O_N defect (level 7) - a close neighbour of the ionized ($V_{Al}-O_N$) center. Recombination of the ($V_{Al}-O_N$)⁺ and (O_N)⁻ centers with emission of a light quantum ($h\nu_{lum}$) results in appearance of the 400 nm emission band.

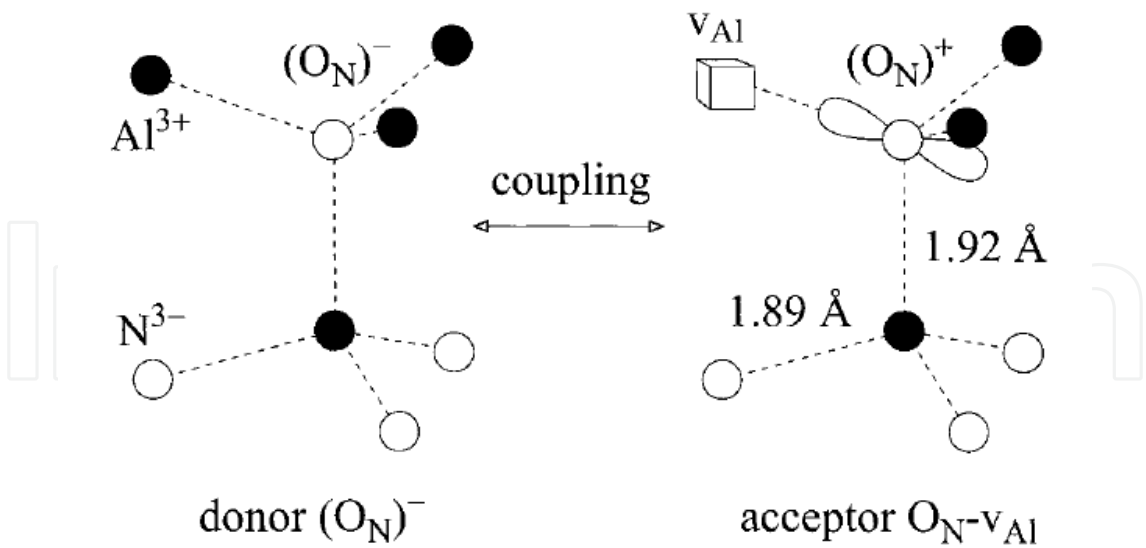


Fig. 4. Model of the coupled donor and acceptor pairs in AlN ceramics (Schweizer et al., 2000)

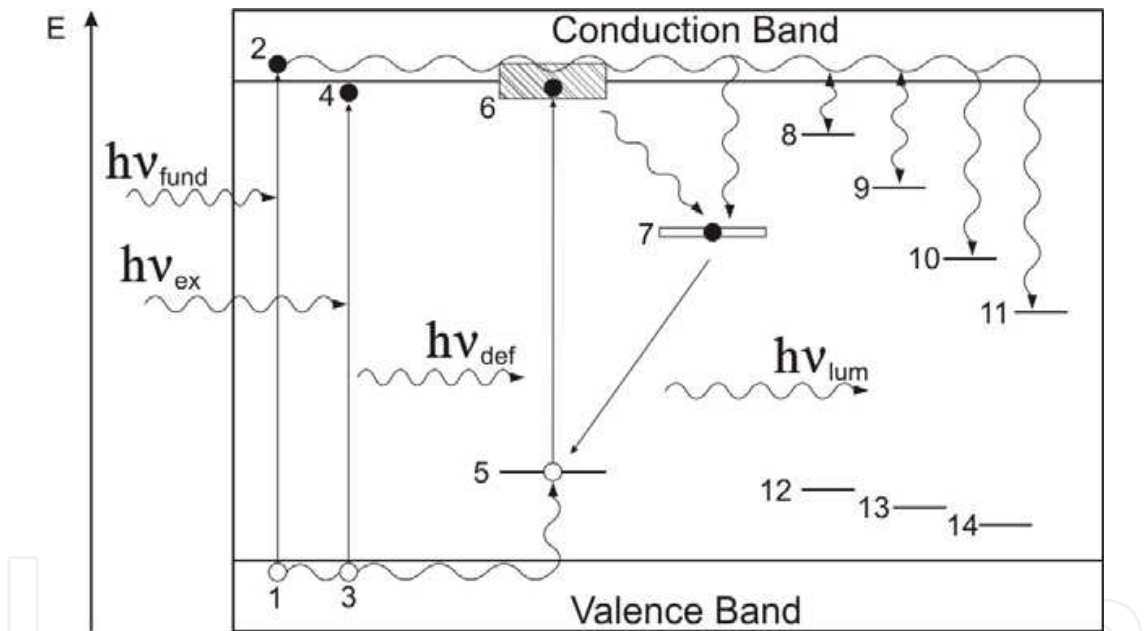


Fig. 5. Energy band diagram of AlN (Berzina et al., 2009). Explanation is given in the text

An electron from the conduction band can be repeatedly recaptured and released by trapping centers, before finally being trapped by O_N defect, thus causing delay of emission rise under continuous excitation with 245 nm, shown in Fig.3.

The similar recombination process can occur under irradiation with light from the fundamental absorption edge region, corresponding to electron-hole pair ($h\nu_{fund}$) or exciton ($h\nu_{ex}$) generation. In this case energy is transferred from host lattice to oxygen-related defects resulting in formation of $(v_{Al}-O_N)^+$ and $(O_N)^-$ centers and 400 nm emission.

The 480 nm subband is also connected with oxygen impurity, which most probably is a part of a complex defect. Tentatively 480 nm emission is ascribed to recombination luminescence with participation of $(v_{Al}-2O_N)$ center (Nappe et al., 2009 and references therein). Such centers are comprised of two close oxygen ions substituting for nitride ion and an aluminum

vacancy. In the energy band diagram the corresponding level is not shown, though it is clear that it should be located a little higher than that of ($v_{\text{Al}}\text{-O}_{\text{N}}$) center and participate in similar processes. Our studies of nanostructured AlN (Berzina et al., 2009 and references therein) have shown that contribution of the 480 nm into the total UV-blue emission increases when size of AlN grains diminishes, and hence, specific surface area expands. It allows supposing that these oxygen-related defects responsible for the 480 nm emission band are located mainly on surface. Besides, the relative increase of the 480 nm band was observed in the samples of AlN ceramics after implantation of oxygen ions (Trinkler et al. 2007a, 2007b). Ion implantation causes damage of the surface layers of AlN and increases oxygen concentration, thus making generation of ($v_{\text{Al}}\text{-2O}_{\text{N}}$) center more probable compared to untreated samples.

3.2 Manganese-related emission

The 600 nm band was observed in PL, afterglow and TL emission spectra of all studied samples of AlN ceramics. Our high resolution measurements, illustrated by Fig. 6 show the presence of fine structure, which can be distinguished at room temperature (RT) and becomes more clearly seen at low temperature. This fine structure is characterized with equidistant peaks with separation energy around 20 meV. This emission band usually is interpreted as luminescence of tetravalent manganese ion Mn^{4+} substituting for Al ion, and equidistant peaks are ascribed to phonon replicas. For the first time this band was observed and interpreted in (Karel et al., 1966) and later studied in other works (Benabdesselam et al., 1995). However, some authors (Miyajima et al., 2006) basing on the results of X-ray absorption fine structure measurements, state that this band is caused by Mn ion having charge between +2 and +3. Other interpretations of the band ascribed to intrinsic defects of AlN are also found in literature, for example, defects formed from nitrogen vacancies (v_{N}) and excess Al (Sarua et al., 2003).

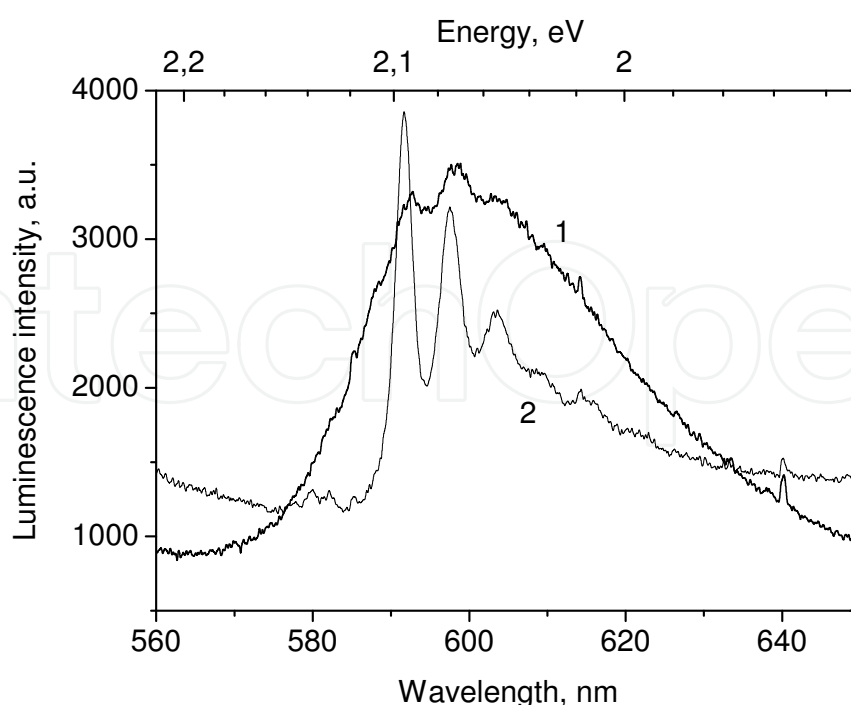


Fig. 6. 600 nm emission band of AlN ceramics measured under excitation wavelength 243 nm at temperature 300 K (1) and 8 K (2)

Excitation spectrum of this emission band is shown in Fig. 7. together with that of 400 nm band. Besides the fundamental absorption edge at 200 nm two excitation bands at 255 and 400 nm are observed. The latter excitation band covers the spectral region of the UV-blue emission band; this results in reabsorption and conversion of UV light into red light. Presence of the 600 nm band in afterglow and TL emission spectra confirms that the corresponding luminescence centre also participates in recombination process.

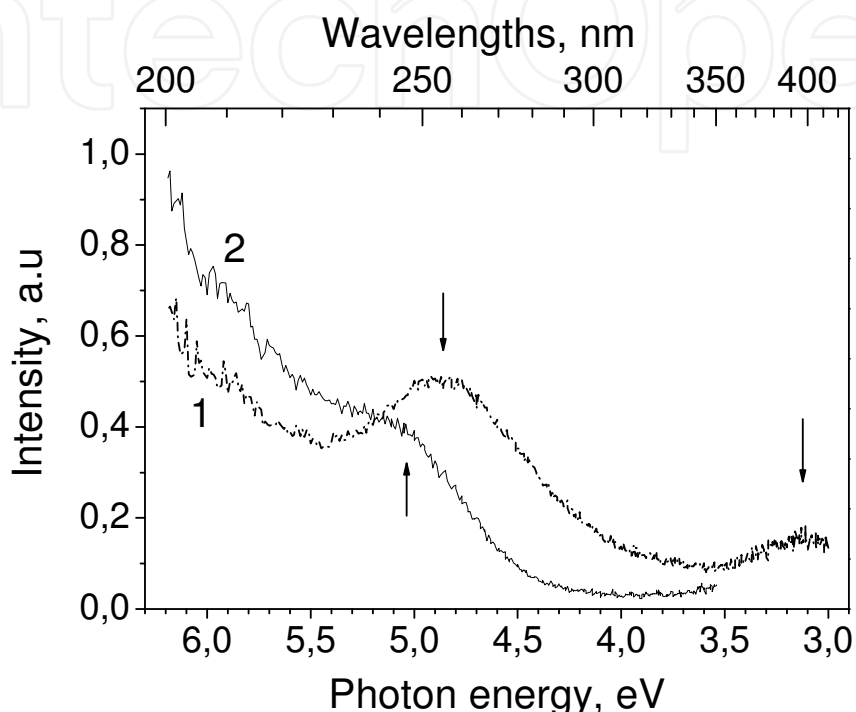


Fig. 7. Excitation spectra of 600 nm band (1) and 400 nm band (2) of AlN ceramics at 300 K

3.3 Other minor PL bands

Other PL luminescence bands observed in AlN ceramics are connected with other uncontrolled impurities. They are the following: a minor band at 700 nm, excited at 280 and 400 nm excitation bands and tentatively ascribed to chromium impurity (Nappe et al., 2011 and references therein) and an infrared band around 1000 nm, connected with iron impurity. At low temperatures the 1000 nm emission band reveals fine structure seen at Fig.1, which is explained as 3d-3d transition ${}^4T_1(G) \rightarrow {}^6A_1(S)$ of Fe^{3+} ion substituting for Al in a regular site and its phonon replicas (Baur et al., 1994).

Summarising the data on PL of AlN ceramics, a conclusion can be drawn that the observed spectral properties of this material are determined by presence of uncontrolled impurities – oxygen, manganese, iron and probably chromium, which form luminescence centres taking part in inter-center and recombination luminescence.

4. AlN ceramics as potential material for solid state dosimetry

There is a number of materials widely used for TL dosimetry as thermoluminescence detectors (TLD) of ionizing radiation, such as $LiF:Mg,Ti$; $LiF:Mg,Cu,P$ and $Al_2O_3:C$. $Al_2O_3:C$

is used also as an effective OSL dosimeter of UV light. Nevertheless a search for new prospective dosimetric materials continues. One of such new dosimetric materials could become AlN ceramics due to its properties revealed under exposure to ionizing radiation and UV light.

As it has been already mentioned irradiation of AlN ceramics causes not only the immediate response to irradiation in luminescence form, but also provides the delayed response in the form of optically and thermally stimulated luminescence. Both TL and OSL processes may be applied in dosimetry for recovering the received radiation dose. Processes of stimulated luminescence in AlN have been studied already before our works (Tale et al., 1982; Benabdesselam et al., 1995). Our studies of the processes of storage and release of radiation induced luminescence signal in AlN ceramics began in 90th and continues up to now. We have found that AlN ceramics is sensitive both to ionizing radiation and UV light, producing TL and OSL response in each case. Properties revealed by AlN ceramics after preliminary irradiation with ionizing radiation (X, β , γ rays) and UV light are similar, but they have also some differences. They will be discussed individually according to irradiation type.

4.1 Stimulated luminescence processes induced by ionizing radiation

4.1.1 Thermoluminescence induced by ionizing radiation

There are several important TL characteristics of material, which determine possibility of its practical application in the area of solid state dosimetry: intensity of TL signal (or in other words sensitivity of material to irradiation), characteristics of TL glow curve, TL emission spectrum, need for additional treatment for use and reuse of a sample, linearity of the dose response, stability of the stored signal and others.

TL properties of AlN ceramics induced by ionizing radiation were studied in comparison with other widely known TLD using the same experimental conditions and irradiation doses (Trinkler et al., 1998). Particularly, it was found that AlN ceramics exhibits amazingly high TL sensitivity. Thus, after irradiation with beta rays ($^{90}\text{Sr}/^{90}\text{Y}$ beta source) for a typical routine read out procedure with the Riso TL reader using a heating rate 10 °C/s the ratio of the TL lightsum (sum of recorded electronic counts) per unit detector mass and radiation dose constitutes 54:27:7:1 for AlN ceramic sample, LiF:Mg,Cu,P, $\text{Al}_2\text{O}_3\text{:C}$ and LiF:Mg,Ti, respectively, see Fig.8.

The TL glow curve of AlN ceramics is characterized with one intensive broad peak extending up to 500 °C, see Fig.8, curve 1. The thermal position of the peak maximum varies from 200 to 300 °C depending on heating rate. No difference in glow curve was observed whether beta particles, γ -rays or X-rays were used for irradiation. The TL signal is completely erased during a single reading using a heating temperature up to 500 °C. Thus no additional annealing or other procedure is necessary for re-use of the sample. A repeatability test showed that reduction of sensitivity after 10 successive irradiation-TL reading cycles was less than 1 %.

Dose response curve of AlN ceramics was measured in dose range $5 \cdot 10^{-3}$ - $5 \cdot 10^{-2}$ mGy (irradiation with ^{60}Co source) in comparison with other mentioned TLD. The curves shown in Fig.9 were obtained by Alnor TL reader using a nitrogen temperature of 300 °C for all samples except for LiF:Mg,Cu,P, which was heated up to 260 °C. AlN ceramics sample revealed linear dose response in the range of five orders of magnitude, like other acknowledged TLD materials, which must be confessed as a very good result.

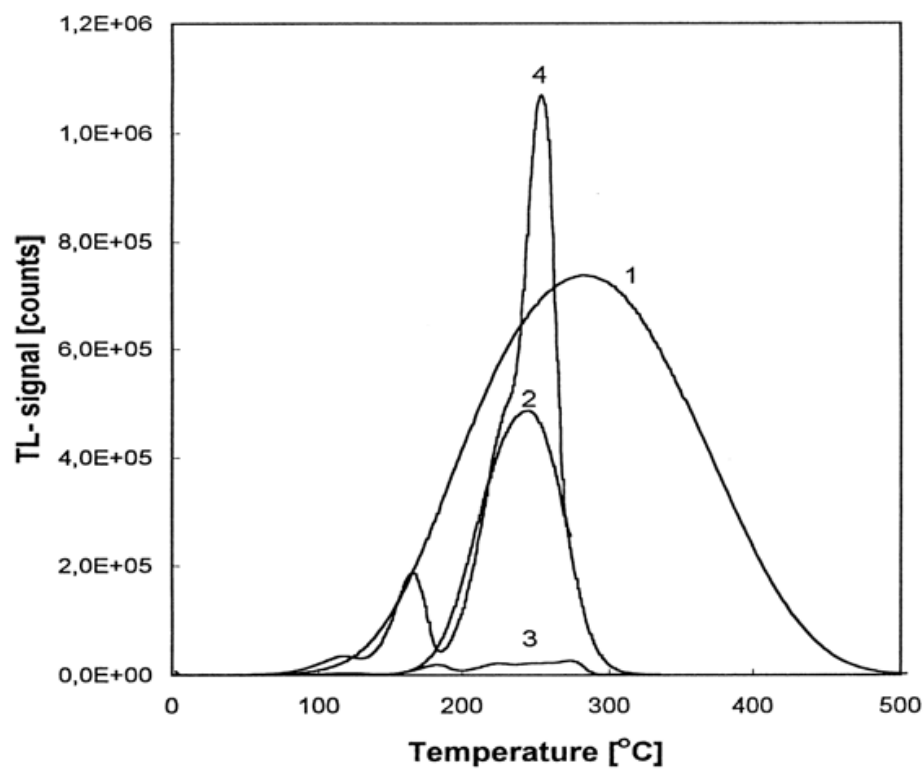


Fig. 8. Glow curves of different types of TL dosimeters irradiated with 28 mGy beta radiation: 1 – AlN ceramics; 2 - Al₂O₃:C; 3 - LiF:Mg,Ti, 4 - LiF:Mg,Cu,P (Trinkler et al, 1998)

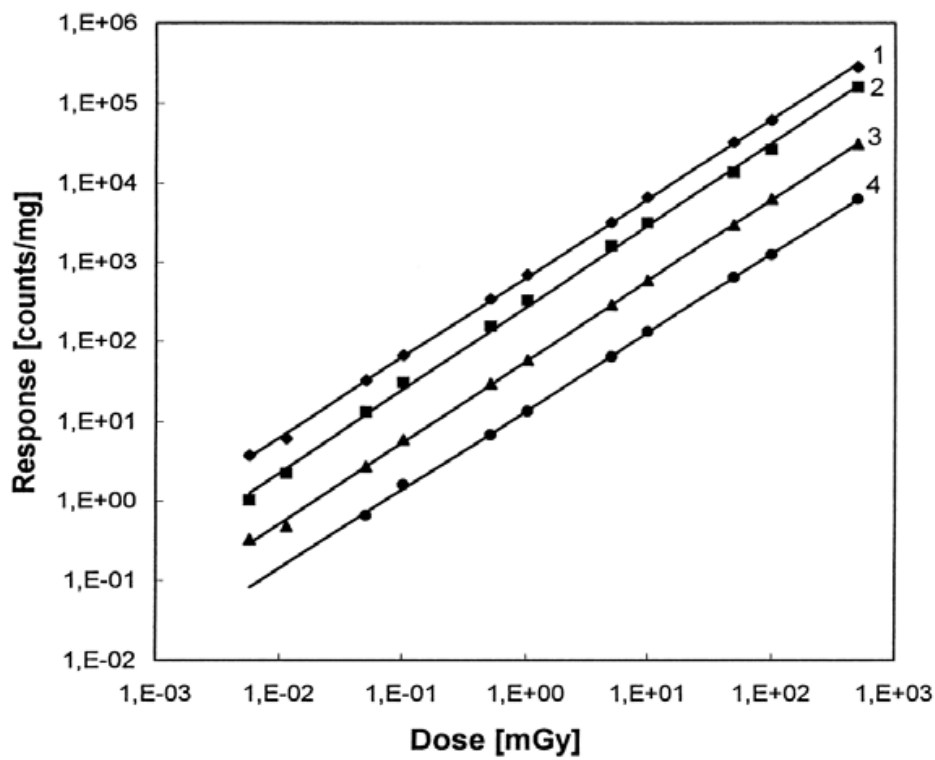


Fig. 9. Gamma ray (⁶⁰Co) dose response of AlN ceramics (1), LiF:Mg,Cu,P (2), Al₂O₃:C (3) and LiF:Mg,Ti (4) obtained with Alnor hot-nitrogen heated TL reader

TL emission detection region was limited by spectral region of 300-500 nm, in order to discriminate thermal glow emission of the heater, which is observed at high temperatures in the red region. In the same time it is an optimal spectral region for detection with usual photoelectron tubes and other light detectors. In this spectral range AlN emission was observed with a maximum position around 400 nm, which shifted to longer wavelengths with rise of heating temperature. The observed emission corresponds to UV-blue luminescence band of AlN, which is ascribed to oxygen-related defects. Other luminescence bands of AlN ceramics can not be observed in these experimental conditions. Influence of heating rate on TL signal for AlN ceramics was measured for heating rates from 0.5 to 20 °C/s in comparison with TLD Al₂O₃:C, whose response is critically sensitive to heating rate, hampering routine reading measurements of this TLD and resulting in uncertainty in the dose measurements if significant fluctuations of heating rate occur. Contrary to Al₂O₃:C, TL response of AlN sample shows only a small influence on heating rate, as it is illustrated in Fig.10.

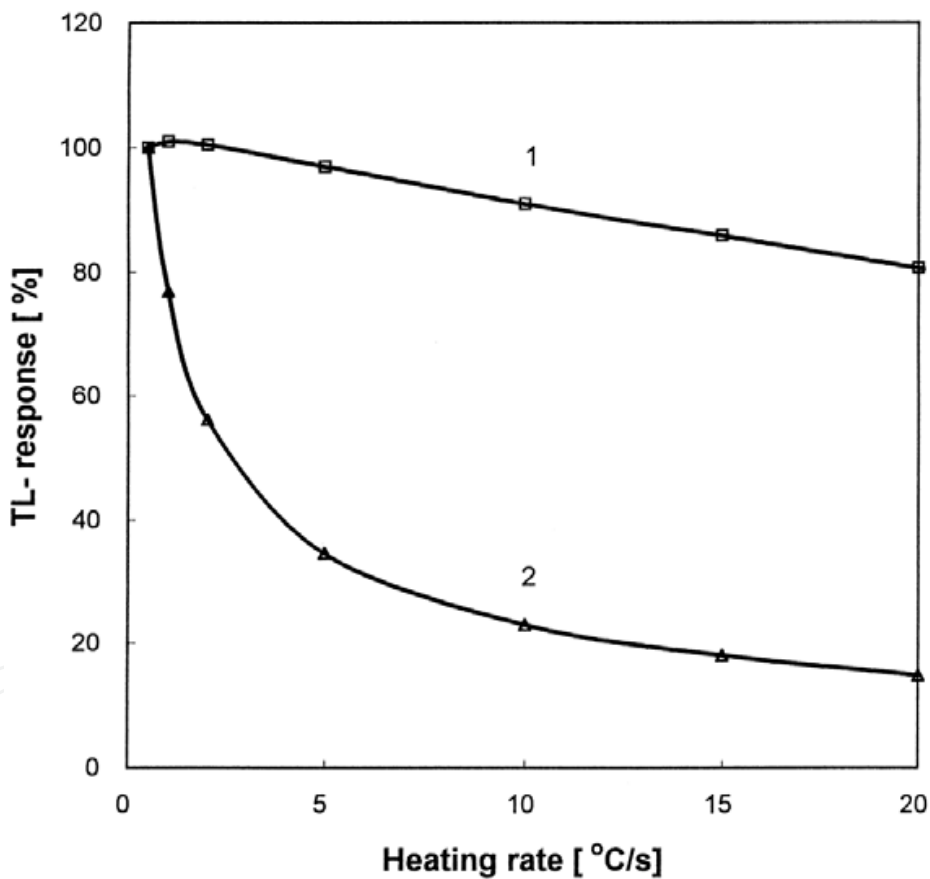


Fig. 10. Influence of heating rate on the TL response of AlN ceramics (1) and Al₂O₃:C (2) irradiated with 28 mGy beta radiation

Considerable fading of the TL signal was observed for AlN ceramics sample on storage at RT. Change of TL glow curve on storage at RT during 114 hours is illustrated in Fig.10. The TL signal is decreasing mainly due to disappearance of the low temperature part of the glow curve, but the high temperature part is also decreasing considerably. Different pre-heat procedures were tried varying preheat temperature and duration: as a result the fading rate

was decreased but not eliminated. However, at the same time the TL yield was essentially reduced by this procedure.

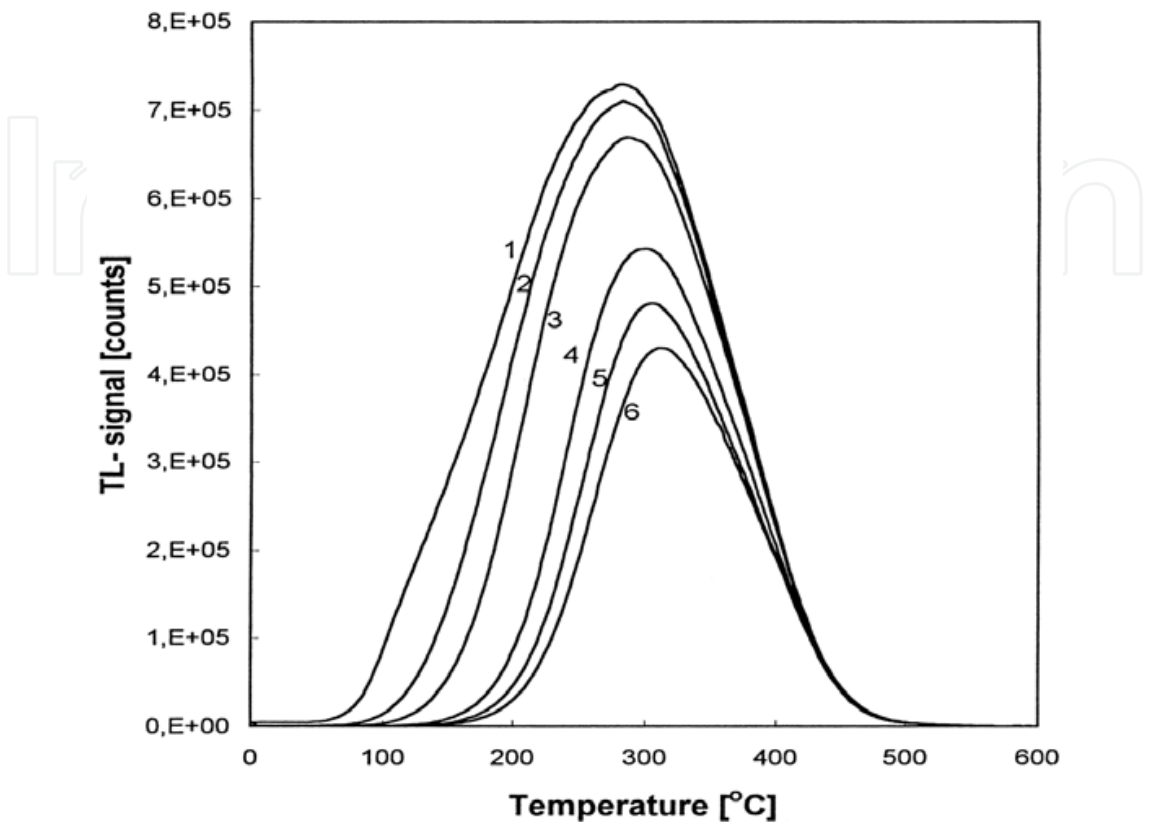


Fig. 11. TL glow curves of AlN samples recorded for different storage periods at RT after irradiation with 42 mGy beta radiation: just after irradiation (1); after a storage period of 0.17 (2); 1 (3); 24 (4); 72 (5) and 114 (6) hours

Neither the pre-irradiation with high dose (1 kGy of ⁶⁰Co gamma irradiation) with subsequent annealing nor a special procedure of very slow annealing (1 °C/min) resulted in improvement of fading characteristics of AlN ceramics. The pronounced fading of the TL signal in AlN ceramics is a serious obstacle for its application as TLD material.

Sample No	Sintering time (min)	Sintering temperature (°C)	TL response after irradiation (counts.mg ⁻¹)	TL response after 17 h (counts.mg ⁻¹)	Fading (%)	TL peak position (°C)
612	210	1645	1334	920	32	380
592	210	1705	13053	7826	40	310
572	210	1745	27673	14639	47	260
552	210	1780	36165	18160	50	250
541	120	1780	32252	15240	53	250
511	40	1780	12601	3238	74	210

Table 1. Influence of sintering conditions of AlN ceramics on TL properties. The TL response is measured immediately after and 17 h after irradiation with 1.7 R X-rays

An attempt was made to study the effect of ceramics sintering conditions on the fading rate (Trinkler et al., 1999). Samples under investigation were produced from the same initial material varying sintering temperature and time. The results of the study are summarized in Table 1. It was found that rise of the sintering temperature leads to the strong increase of the TL yield and also to a shift of the TL peak position to lower temperature with increasing fading rate. An increase of sintering time at constant sintering temperature also causes a rise of the TL yield, but in this case the thermal peak shifts to higher temperature, and hence, the fading rate decreases. The reasons why the TL peak shifts may be explained by generation of oxygen-related defects of different types, whose balance depends on sintering conditions. The optimal sintering conditions are found using the lowest sintering temperature and the longest sintering time, but even this procedure does not eliminate completely fading of the TL signal.

4.1.2 Optically stimulated luminescence induced by ionizing radiation

Optically stimulated luminescence is detected as a pulse of luminescence light decaying in time under continuous exposure of stimulation light. An OSL signal bleaches because stimulation light empties trapping levels. Typical OSL decay curve of AlN contains an intensive fast component and a weak slow component. Each of them has its own specific fading rate, fast component fades faster. Intensity of OSL is characterized with a lightsum – integral of electronic counts detected during a pulse up to its complete depletion. The following characteristics of OSL are important for characterization of material and estimation of its potential application as an OSL dosimeter: OSL emission spectrum, OSL stimulation spectrum; linearity of dose response, fading of the stored signal and others.

OSL induced by ionizing radiation in AlN ceramics (Trinkler et al., 1999) was studied using Riso TL/OSL reader, which is not designed for spectral measurements, but at the same time allows comparison of TL and OSL properties of material under the same conditions. Irradiation was performed with beta source, while stimulation was done by infrared and blue light sources, all sources integrated in the reader. Luminescence was recorded in the 300-500 nm range, corresponding to oxygen-related luminescence of AlN.

It was found that OSL sensitivity to ionizing radiation is approximately 40 times lower than TL sensitivity after the same beta dose. Not all the light yield produced by the irradiation can be released by optical stimulation: after the complete optical bleaching a residual TL signal was observed in the 300-500 °C temperature region. Study of the preheat influence showed that OSL is much more sensitive to preheat treatments than TL: after a preheat up to 150 °C during 300 s only 10% of OSL yield is left compared to 65% of TL yield in the same conditions.

The OSL decay curve induced by ionizing radiation has a dominating fast component, and its fading rate is high. It was found that OSL fading characteristics are worse than those of TL: after 150 hours of storage at room temperature only 10% of the initial OSL response is left compared with 45% of the TL response.

All the above mentioned results show that only a part of the light yield produced by ionizing radiation can be released by optical stimulation. The light-sensitive part of the stored signal can be ascribed to the trapping of the charge carriers in the shallowest trap levels located in the band gap of AlN, while the rest part of the stored signal is more stable due to trapping of charge carriers on deeper levels, which can be emptied only by heating up to sufficiently high temperatures.

It may be concluded that AlN can not be recommended for use as OSL detector of ionizing radiation because a typical OSL response is much weaker and more unstable than the TL response for the same dose.

4.2 Stimulated processes induced by UV light

Detection of UV radiation doses is an important area of dosimetry. UV radiation usually is divided into three spectral regions namely: UV-C (shorter than 280 nm), UV-B (280-315 nm) and UV-A (315-400 nm). Radiation of UV-C region is used in industry for characterization of materials and products and in disinfection procedures due to its bactericidal effect. UV-B region corresponds to the part of the spectral distribution of the Sun's rays reaching ground level and which is potentially harmful to human beings and other organisms. Uncontrolled exposure of naked human bodies to Sun rays from UV-A region also can cause some problems. Monitoring of UV light intensity and measuring of UV doses is important in all of these regions.

A number of our works is devoted to UV light induced stimulated processes in AlN ceramics (Trinkler et al., 2000, 2001b, 2002). It was found that this material is extremely sensitive to UV radiation producing high response both in TL and OSL. Some experiments were done in comparison with dosimetric material $\text{Al}_2\text{O}_3\text{:C}$, commonly used for UV dose measurements (Akselrod et al., 1990). We have measured full spectral characteristics of UV light induced TL and OSL processes: excitation spectra, emission spectra and stimulation spectra (for OSL), as well as TL glow curves, including 8-300 K temperature region.

4.2.1 Properties of UV light induced TL and OSL compared to those induced by ionizing radiation

A study was done when TL and OSL measurements were performed with AlN ceramics and $\text{Al}_2\text{O}_3\text{:C}$ dosimeter in the same conditions after exposition to ionizing radiation and UV light, simultaneously comparing sensitivity of materials to radiation exposure and effects of different type of radiation on both materials (Trinkler et al., 2000). For this study the Sol-2 lamp in combination with interference filters was used as a UV light source, while TL and OSL response was measured with Riso TL/OSL reader.

The most attractive feature of AlN ceramics is the very high sensitivity to UV radiation, which is demonstrated by Fig.12. The TL response from AlN ceramics irradiated by beta particles is about 20 times higher than that of $\text{Al}_2\text{O}_3\text{:C}$ (curves 1 and 3) and about 6000 times higher in the case of UV irradiation with wavelength 350 nm (curves 2 and 4). On this figure for the used TL yield scale the curve 4 is undistinguishable from the temperature axis. TL signal from the UV dosed AlN ceramics is characterized with a very broad and structureless glow curve (curve 2) with a maximum around 320 °C, which is significantly higher than that for beta irradiated AlN, corresponding to 230 °C (curve 1). A lower fading rate of the integrated TL signal was observed for AlN samples exposed to UV light (40 % fading over 24 h storage) than for samples exposed to beta radiation (66 % fading). This is explained by the shift of the TL curve to the higher temperature.

The TL response of AlN ceramics to UV radiant exposure was obtained by varying both the irradiation time and the irradiance, changing the distance between the sample and the excitation lamp and using sieve filters of different density. Figure 13 shows a linear relationship between the TL yield and UV radiant exposure over at least five decades. The

deviation from the linear slope observed at the highest UV doses is explained by fading effects, due to the relatively long irradiation times required.

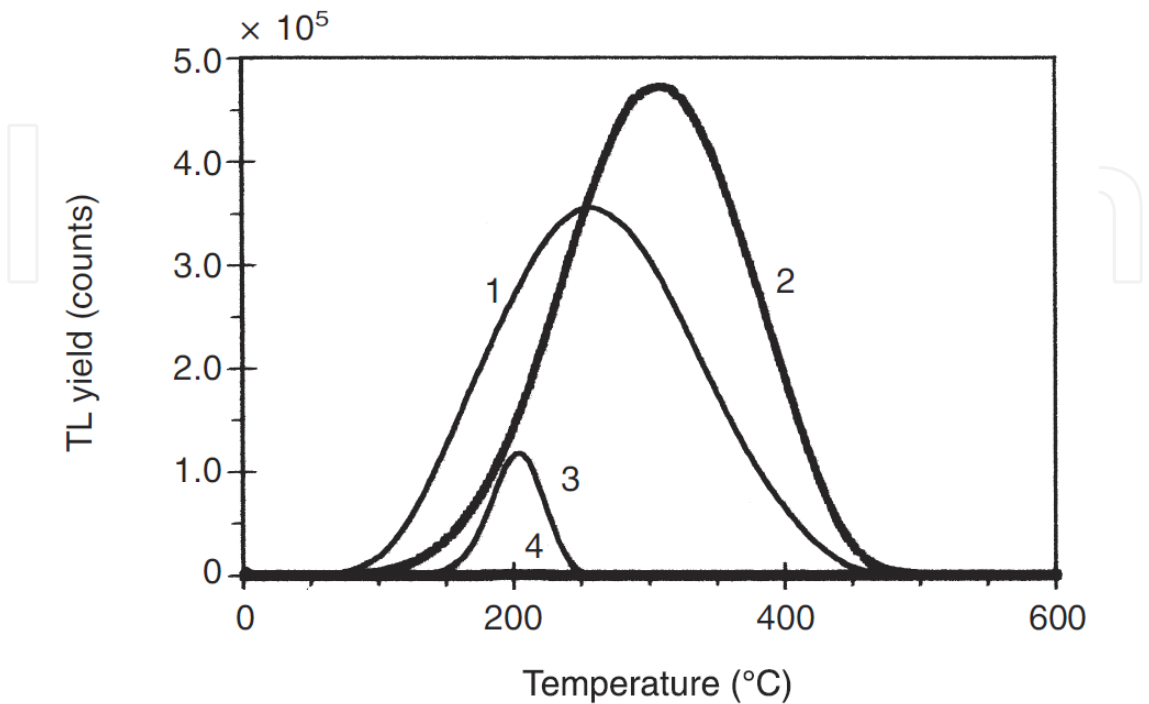


Fig. 12. TL curves obtained from AlN ceramics and Al₂O₃:C after irradiation with 100 mGy beta dose (1 and 3) and 1 min exposure to UV light produced by the lamp Sol 2 and using an interference filter with peak transmission at 350 nm

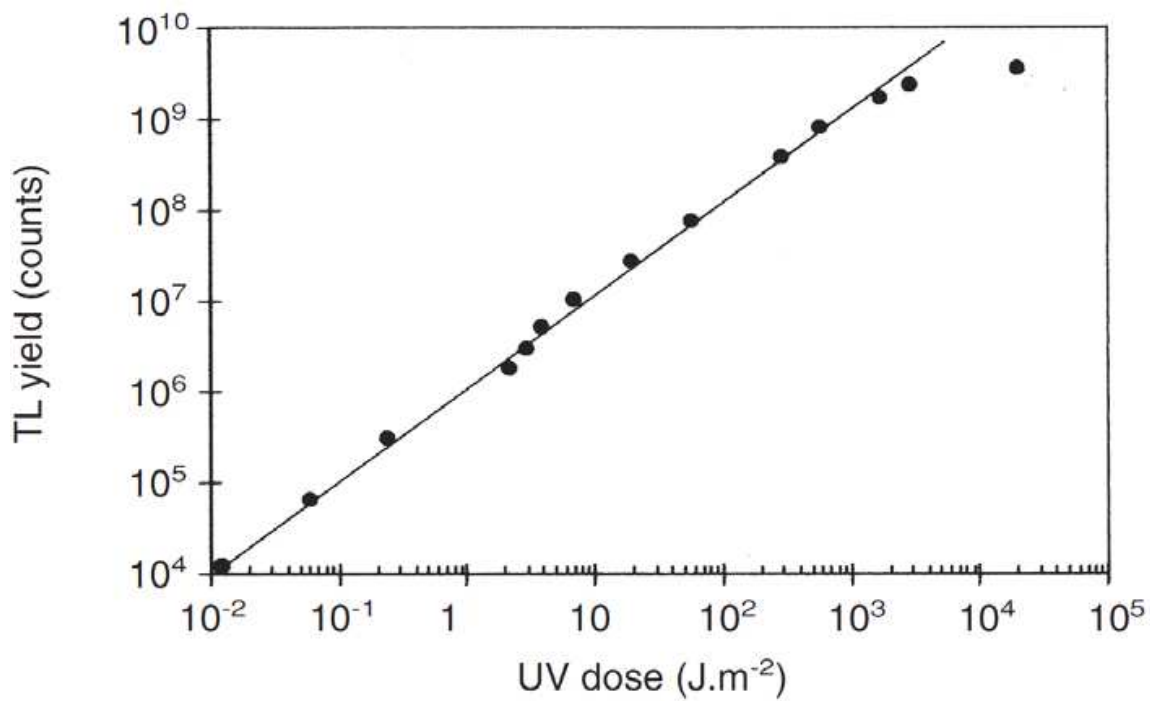


Fig. 13. UV light dose dependence of AlN

The OSL decay curves obtained from AlN and Al₂O₃:C after both beta and UV radiation are shown in Fig.14. In contrast to Al₂O₃:C showing the same shape of decay curves for both type of irradiation (curves 3 and 4), AlN ceramics has two different decay curves: an intensive fast component that dominates in beta-induced OSL (curve 1) and a slow component, which dominates in UV-induced OSL (curve 2). Although the initial OSL intensity of the AlN sample is significantly higher than that of Al₂O₃:C when exposed to beta radiation, this very fast AlN component yields less signal. Alternatively, when irradiating AlN with UV light of 350 nm, its OSL signal is about 60 times higher than that of Al₂O₃:C. Ratio of the UV light induced TL and OSL signals from AlN and Al₂O₃:C depends on the wavelength of UV irradiation, because each of the materials has its own spectral sensitivity, revealed by TL and OSL excitation spectrum. Thus at irradiation 200-230 nm corresponding to the highest sensitivity of Al₂O₃:C is the OSL response of this material is higher than that from AlN, at other wavelength it is lower.

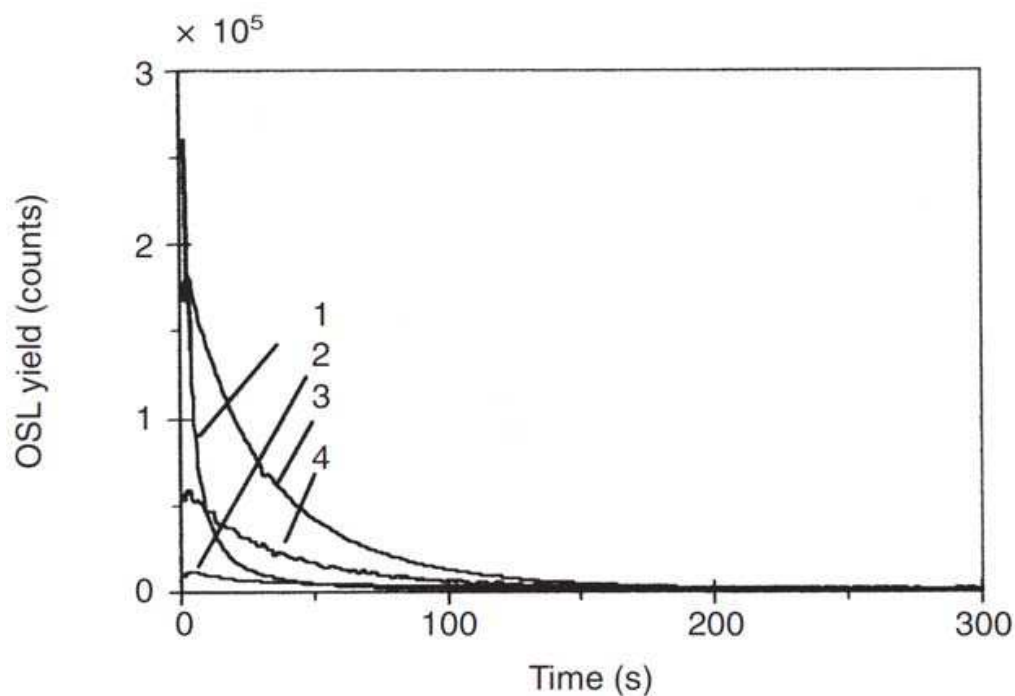


Fig. 14. OSL decay curves obtained from AlN ceramics and Al₂O₃:C after irradiation with 100 mGy beta dose (1 and 3) and 1 min exposure to UV light produced by the lamp Sol 2 and using an interference filter with peak transmission at 350 nm. Stimulation was performed with 470 nm light. Curve 4 is multiplied by a factor of 100

The initial part of the OSL pulse, which consists mainly of the fast component, fades faster during the storage of the dosed sample than the tail of the pulse, consisting of the slow component. That is why the fading effect is higher for the beta induced OSL, which has a dominant fast component of the decay curve: only 10% of the initial response is left after 24 hours of storage. The effect of fading is less pronounced for UV induced OSL having a dominant slow component: 45% of the initial response is left after 24 h.

The properties observed in the UV induced AlN samples such as the peaking of the TL glow curve at a higher temperature, absence of an intensive fast component of the OSL decay curve, lower fading rate of both the TL and OSL signals, assume that the UV radiation

induced stimulated luminescence involves a larger part of deep traps compared to those created by beta radiation. The deeper traps need higher energy for depopulation.

The OSL response dose dependence taken as OSL yield versus UV irradiation time up to 60 min deviates from a linear slope. This is explained by fading of the OSL signal during irradiation and insufficient OSL readout time for the higher doses.

4.2.2 Spectral characteristics of UV induced TL and OSL

Spectral sensitivity of AlN ceramics was determined from excitation spectrum of TL and OSL, which appeared to be similar and covering almost the whole UV region from 200 to 350 nm, with maximum effect at 240-270 nm, corresponding to absorption of oxygen-related centers. This characteristic for OSL process is shown on Fig. 15, curve 1 (Trinkler et al, 2002).

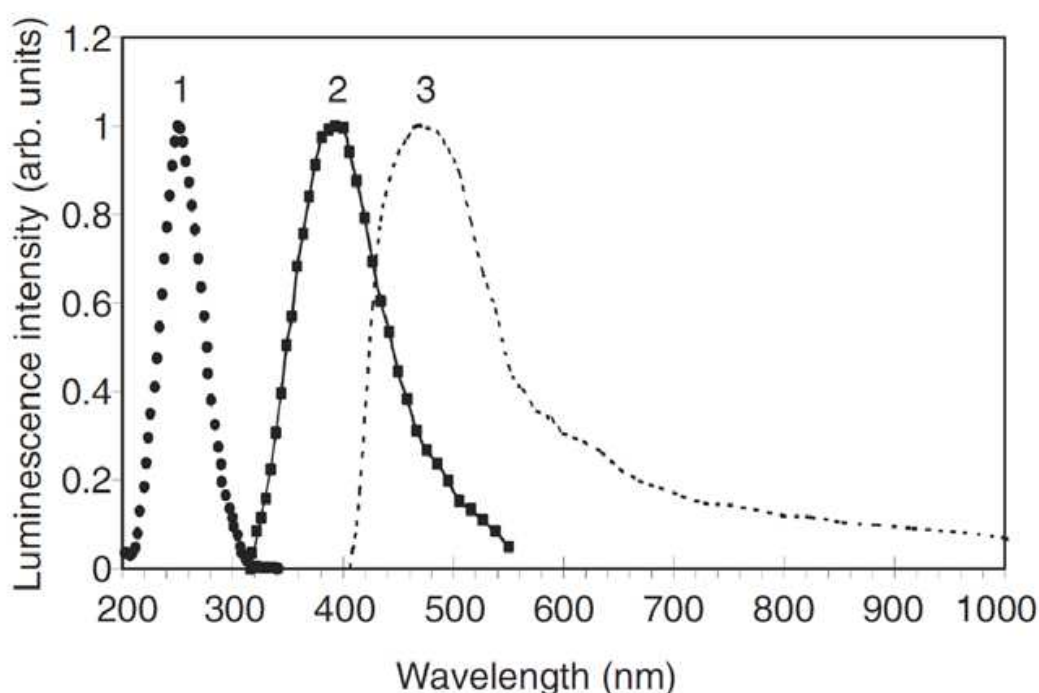


Fig. 15. Spectral characteristics of UV light induced OSL of AlN ceramics: OSL excitation spectrum (1), OSL emission spectrum (2), OSL stimulation spectrum (3)

It is remarkable that spectral sensitivity of AlN is similar with spectral sensitivity of human skin in the 280-340 nm range (see Fig.16), which corresponds to UV-B region of Solar emission potentially dangerous for human beings. This property makes AlN ceramics useful for application as material for personal UV dosimeter.

OSL emission spectrum is presented with the same UV-blue band as PL band ascribed to oxygen-related centers, as it is seen from Fig. 15, curve 2. In order to separate emission and stimulation light the detection region is limited and nothing could be said about presence of long wavelength bands in OSL emission. TL emission spectrum shown on Fig. 17. (Trinkler et al., 2003) also has the same UV-blue band, whose intensity and position of maximum shifts depending on excitation wavelength. Besides, it contains also 600 nm band. TL and OSL emission spectra fall into the 300-600 nm range, which is suitable for detection with common light detectors.

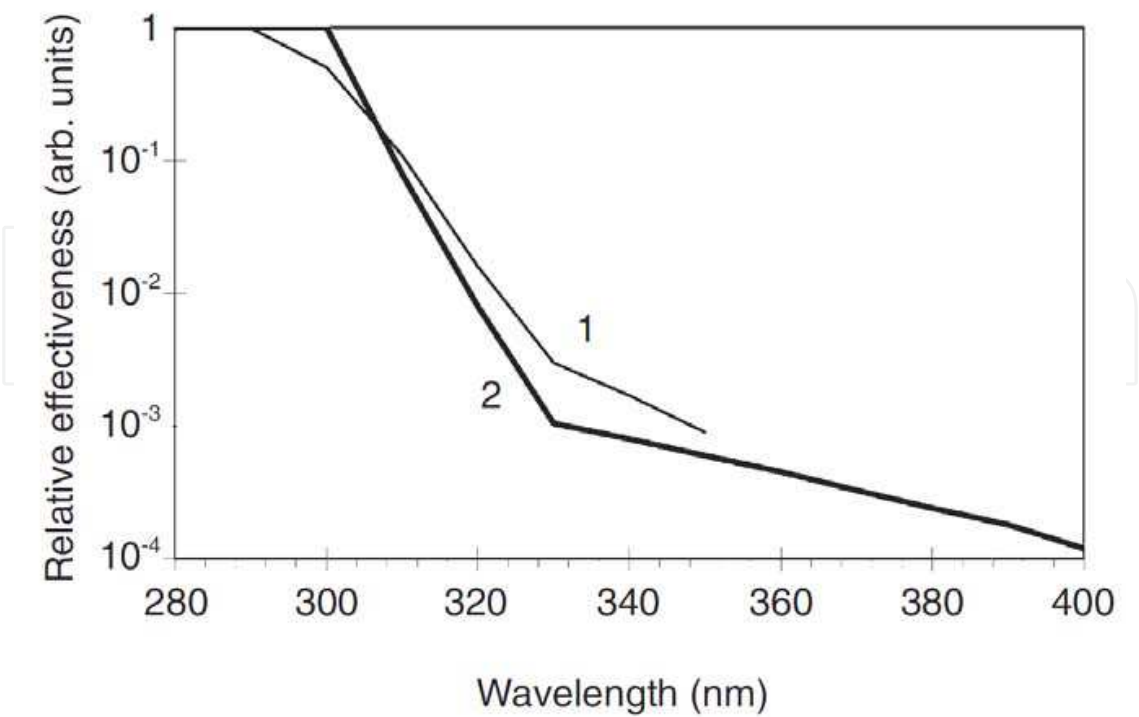


Fig. 16. Comparison of OSL excitation spectrum of AlN ceramics (1) with action spectrum of human erythema (2) (CIE Research Note, 1987)

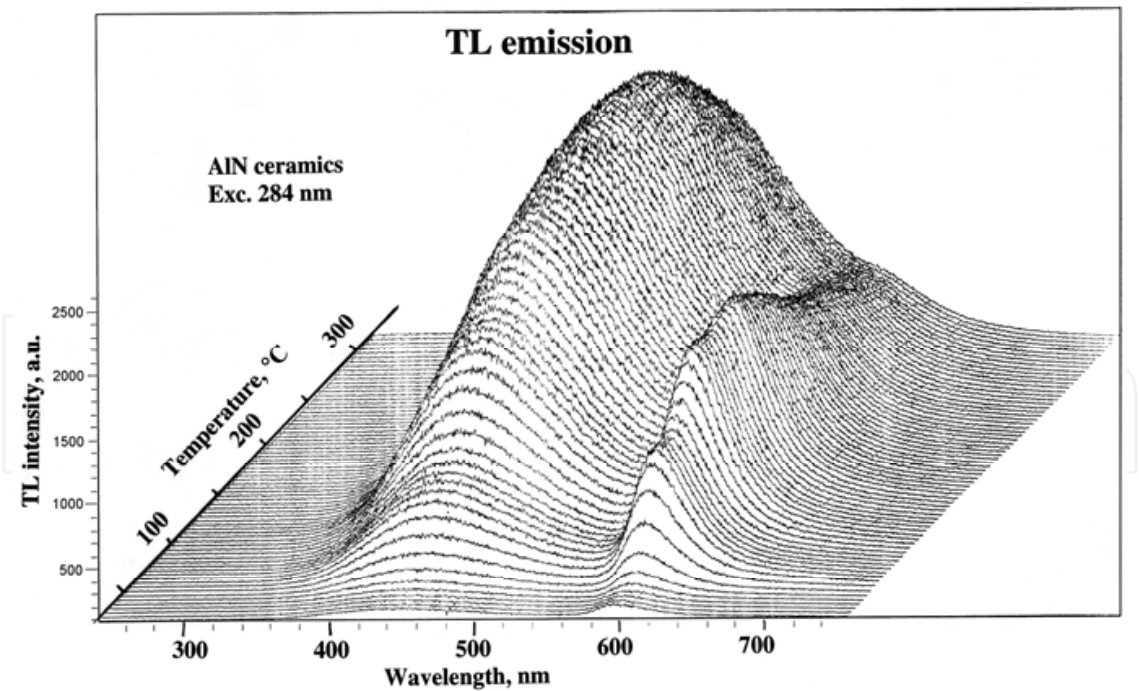


Fig. 17. 3D image of UV light induced (excitation 284 nm) TL emission from AlN ceramics

OSL is characterized also by stimulation spectrum, determined by energy levels of trapping centres, emptied during optical stimulation. For AlN ceramics it extends from 400 up to 1000 nm with an expressed maximum at 500 nm, see Fig.15, curve 3. Large spectral interval and

complex structure of the OSL emission spectrum means that numerous different trap levels participate in the stimulated luminescence process. Most of halogen and incandescent lamps with continuous distribution of emission in combination with glass filters as well as monochromatic LEDs and lasers are suitable for use as stimulation sources of OSL from AlN ceramics.

4.2.3 Use of 480 nm emission band for UV induced TL and OSL

It has been shown already that the oxygen-related UV-blue PL emission band contains two subbands around 400 and 480 nm, each subband having its own excitation spectrum, as shown in Fig.18, curves 1 and 2. The same emission bands at 400 and 480 nm can be distinguished also in TL and OSL emission spectra. Similarly to PL case, each of these bands is characterised with a distinct shape of TL or OSL excitation spectra. The case of TL excitation spectra recording emission at 400 and 480 nm is shown in Fig. 18 (curves 3 and 4). The results on TL and OSL experiments mentioned in previous sections were obtained selecting either the 400 nm emission band or the whole UV-blue band. However, it appeared that selection of the 480 nm for detection of stimulated emission results in better parameters of the TL and OSL processes (Trinkler et al, 2007a, 2007b).

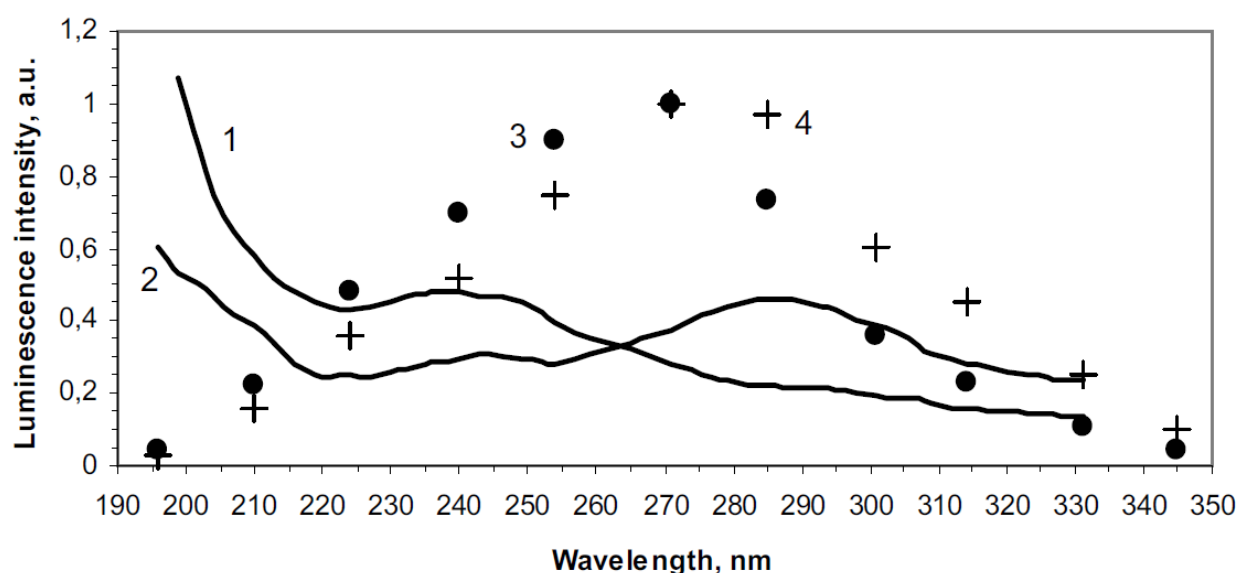


Fig. 18. Excitation spectrum of PL (1, 2) and TL (3, 4) of AlN ceramics recording emission at 400 nm (1, 3) and 480 nm (2, 4)

It was found that intensity and shape of TL curves measured in the same conditions depend on the selected excitation and emission wavelength. Two peaks are distinguished in TL curves: those at 80 and 220 °C (see Fig.19). The low temperature peak is better pronounced selecting 400 nm emission under irradiation in its characteristic excitation band (curve 1), while the high temperature peak appears for selection of 480 nm emission after excitation in the long wavelength region (curve 4). Other curves (2 and 3) contain both peaks due to overlapping of the emission bands. The higher temperature of the TL glow peak implies the lower fading rate of the stored signal. Indeed, measurement of TL signal after one hour of storage had shown 50 % of the initial yield of the TL response at 400 nm emission excited at 245 nm contrary to 80 % of that for 480 nm emission excited at 315 nm.

Correlation of emission bands with the definite TL glow peaks speaks in favor of pair distribution of trap centers and recombination centers, as it was approved already for $(V_{Al}-O_N)^+$ and $(O_N)^-$ centers, responsible for the 400 nm band. The trap centers responsible for the 480 nm emission evidently are more stable, than those participating in the 400 nm emission, and the corresponding TL and OSL signal fades slower. Similar effect was observed for the OSL process (Trinkler et al., 2007b): after one hour storage selection of the 480 nm band provided 40% of the initial value of the OSL yield versus 18 % for selection of 400 nm band.

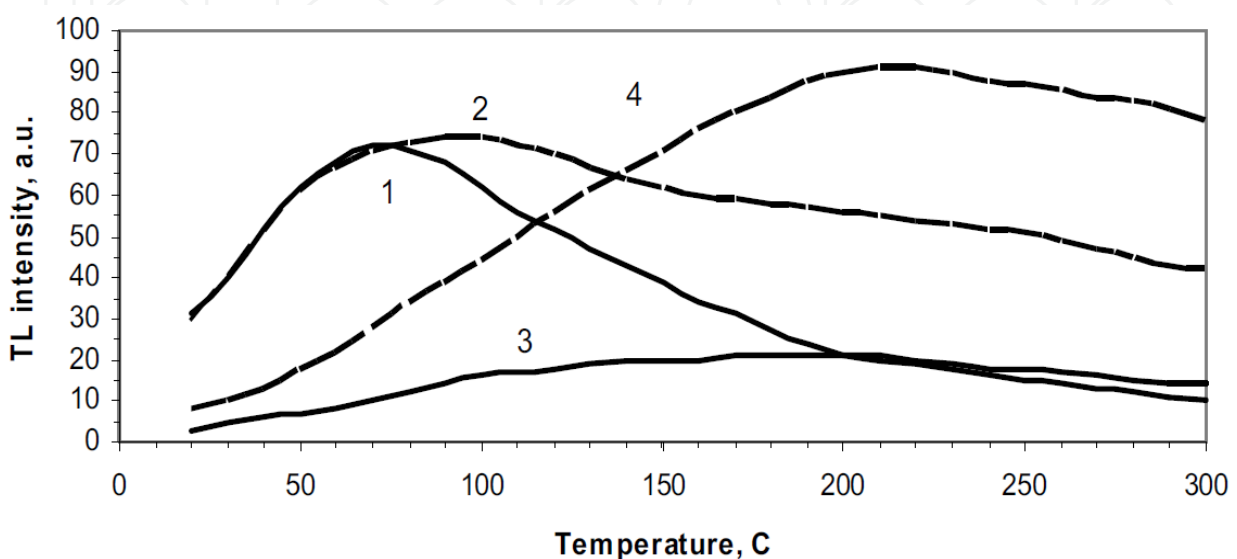


Fig. 19. TL curves of AlN ceramics after UV light irradiation at 245 nm (1, 2) and 315 nm (3, 4) detecting emission at 400 nm (1, 3) and 480 nm (2, 4)

We have done a special study of stimulated processes in AlN ceramics subjected to ion implantation with oxygen ions. It was found that after such treatment relative contribution of the 480 nm band into the total emission spectrum increases. In the same time this procedure provides very little improvement in the intensity and stability of the OSL signal, but gives some improvements of the dosimetric characteristics for TL.

From the results obtained it follows that for UV dosimetry applications it is better to use the 480 nm emission band, since the response signal is more stable than that for the 400 nm band and its excitation spectrum falls in the UV-B region, which is the detection range of practical interest. Comparing different types of dosimetric applications of AlN ceramics it should be recognized that OSL method is less suitable because of a higher rate of decrease of the signal at room temperature.

4.2.4 TL in the low temperature region

Recently we have done experiments on TL measurements of AlN ceramics at low temperature. The sample was irradiated with UV light of different wavelengths at 8 K. TL signal was recorded during heating of the sample up to 300 K. Two glow curves corresponding to the main oxygen-related bands are shown in Fig. 20.

The common feature of all glow peaks is a peak at 60 K, at further rise of temperature behavior of glow curves is different until 270 K, when both curves begin to rise. This rise is the beginning of the main TL peaks, whose maxima were observed at 80 °C (353 K) for 400 nm emission band and 220 °C (493 K) for 480 nm emission band. It means that room

temperature 20 °C (293 K) is sufficiently high to start the spontaneous thermoluminescence process without any external heating. This process will continue until complete depletion of the trapped charge carriers. Storage of the dosed samples at room temperature will lead to the fading of the stored TL and OSL signal.

Thermal region of the main peaks is determined by the set of trapping centres present in AlN ceramics. The fading problem could be solved if the dosed AlN samples are stored at reduced temperature (around 250-260 K). Another way to eliminate fading is to introduce impurities providing deep trapping levels in the energy band diagram of AlN, which are stable at room temperatures. Further practical studies of this phenomenon are planned.

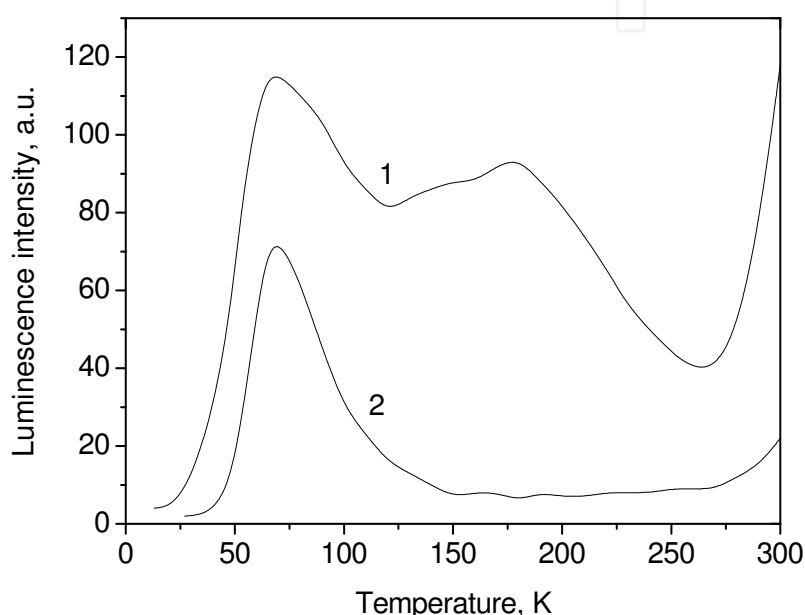


Fig. 20. TL glow curves of AlN irradiated at 8K: (1) excitation 243 nm, emission 400 nm, (2) excitation 298 nm, emission 500 nm

5. Conclusions

AlN ceramics is a wide-gap material whose spectral properties are determined by presence of uncontrolled impurities and intrinsic defects, the main role played by oxygen-related defects. The fulfilled investigations show that AlN ceramics is a material, highly sensitive to irradiation with both ionizing radiation and UV light. The dose of the obtained irradiation can be retrieved using TL and OSL method. In many aspects AlN ceramics outperforms other actually used TL and OSL dosimeters. However, this material has an important drawback, hampering its practical application in dosimetry area – it is high fading rate of the signal during storage at room temperature.

Different measures have been tried to diminish the effect of TL or OSL signal fading, such as optimization of ceramics sintering conditions, use of preheat procedure, detection of the definite emission band (480 nm) and oxygen ion implantation. These measures helped to slow down, but not to eliminate the fading process, which is determined by intrinsic properties of AlN ceramics. That is why at present AlN is not offered for practical

application in the area of solid state dosimetry. The further studies of this potentially perspective material are planned.

6. Acknowledgement

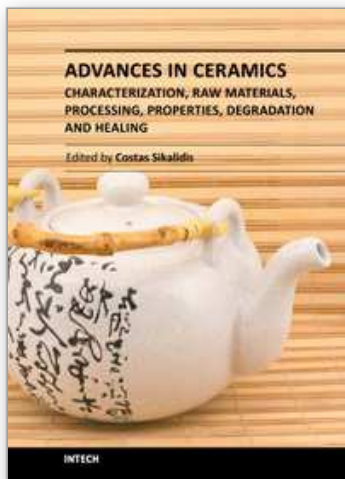
This work was supported by ERAF Project 2010/0204/2DP/2.1.1.2.0/10/APIA/VIAA/010.

7. References

- Akselrod, M.S. ; Kortov, V.S. ; Kravetsky, D.J & Gotlib, V.I. (1990). High sensitive thermoluminescence anion-defective $\text{Al}_2\text{O}_3:\text{C}$ single crystal detector. *Radiation Protection dosimetry*, Vol 32, Nos. 1-4, (April 1990), pp. 15-29, ISSN: 0144-8420
- Baur, J. ; Maier, K. ; Kunzer, M. ; Kaufman, U. & Schneider, J. (1995). Determination of the GaN/AlN band discontinuities via $(-/0)$ acceptor level of iron. *Materials Science and Engineering B*, Vol. 29, No. 1-3, (January 1995), pp. 61-64 ; ISSN: 0921-5107
- Benabdesselam, M.; Iacconi, P.; Lapraz, D.; Grosseau, P. & Guilhot, B. (1995). Thermoluminescence of AlN – Influence of synthesis processes. *J. Phys. Chem.*, Vol. 99, No. 25, (June 1995), pp. 10319-10323, ISSN: 1089-5639
- Berzina, B. ; Trinkler, L. ; Sils, J. & Palcevskis, E. (2001). Oxygen-related defects and energy accumulation in aluminum nitride ceramics. *Rad. Eff. & Def. In Solids*, Vol. 156, No.1, (January 2001), pp. 241-247, ISSN: 1029-4953
- Berzina, B. ; Trinkler, L. ; Sils, J. & Atobe, K. (2002). Luminescence mechanisms of oxygen-related defects in AlN. *Rad. Eff. & Def. In Solids*, Vol. 157, No. 6-12, pp. 1089-1092, (January 2001), ISSN: 1029-4953
- Berzina, B. ; Trinkler, L. ; Jakimovica, D. ; Korsaks, V. ; Grabis, J. ; Steins, I. ; Palcevskis, E. ; Belluci, S. ; Chen, L.–Ch. ; Chattopadhyay, S. & Chen K.-H. (2009). Spectral characterisation of bulk and nanostructured aluminum nitride. *Journal of Nanophotonics*, Vol. 3, 031950, (December 2009), pp. 1-16, ISSN: 1934-2608
- CIE (International Commission on Illumination) Research Note (1987). A reference action spectrum for ultraviolet induced erythema in human skin. *CIE Journal* Vo. 6, No. 1, (January 1987), pp. 17-22 ; ISSN: 0252-9246
- Harris, R.A.; Youngman, R.A. & Teller, R.G. (1990). On the nature of the oxygen-related defects in aluminum nitride. *J. Mater. Res.*, Vol. 5, No. 8, (August 1990), pp. 1763-1773, ISSN: 2044-5326
- Karel, F.; Pastrnak, J.; Hejduk, J. & Losik, V. (1966). Fine structure of emission spectra of the red AlN:Mn luminescence. *phys. stat. sol. (b)*, Vol. 15, No. 2, (February 1966), pp. 693-699, ISSN: 0370-1972
- Miyajima, T.; Kudo, Y.; Uruga, T. & Hara, K. (2006). Analysis of the local structure of AlN:Mn using X-ray absorption fine structure measurements. *phys. stat. sol. (c)*, Vol.3, No. 6, (May 2006), pp. 1742-1745, ISSN: 1862-6351
- Nappe, J.C.; Grosseau, Ph.; Benabdesselam, M., Beauvy, M. & Guilhot, B. (2009). Characterization of aluminum nitride material under swift heavy ion irradiations. Proceedings of the 11 th ECERS conference, 2009. *11th International Conference and Exhibition of the European Ceramic Society*, pp. 1105-1108, ISBN:9788360958544, Cracow, Poland, May 21-25, 2009
- Nappe, J.C.; Benabdesselam, M.; Grosseau, Ph. & Guilhot, B. (2011). Effect of swift heavy ion irradiations in polycrystalline aluminum nitride. *Nuclear Instruments and Methods in*

- Physics Research Section B: Beam Interactions with Materials and Atoms*, Vol. 269, No. 2, (February 2011), pp. 100-104; ISSN: 0168-583X
- Palcevskis, E. ; Berzina, B. ; Trinkler, L. ; Ulmanis, U. & Mironova-Ulmane, N. (1999). Ceramics from fine plasma processed AlN powder, sintering and properties. *Latvian Journal of Physics and Technical Sciences*, No.1, (February 1999), pp. 34-51, ISSN: 0868-8257
- Palcevskis, E. ; Jakobsen, L. ; Trinklere, L. & Ulmanis, U. (1997) . Ceramics from fine plasma-processed AlN powder. *Key Engineering Materials*, Vols. 132-136, (1997), pp. 185-188, ISSN: 1662-9795
- Sarua, A.; Rajasingam, S.; Kuball, M.; Garro, N.; Sancho, O.; Cros, A.; Cantarero, A.; Olguin, D.; Liu, B.; Zhuang, D. & Edgar, J. (2003). Effect of impurities on Raman and photoluminescence spectra of AlN bulk crystals. *Materials Research Society Symposium – Proceedings*, 798, (May 2003), pp. 297-302, ISSN: 0272-9172
- Schweizer, S.; Rogulis, U.; Spaeth, J.-M.; Trinkler, L. & Berzina, B. (2000). Investigation of oxygen-related luminescence centres in AlN ceramics. *phys. stat. sol. (b)*, Vol. 219, No. 1, (January 2000), pp. 171-180, ISSN: 0370-1972
- Slack, G.A. (1973). Nonmetallic crystals with high thermal conductivity. *J. Chem. Phys. Solids*, Vol. 34, No. 2, (February 1973), pp. 321-335, ISSN : 0022-3697
- Tale, I. & Rosa, J. (1984). Fractional glow technique spectroscopy of traps in heavily doped AlN:O. *phys. stat. sol.(a)*, Vol. 86, No.1, (January 1984), pp. 319-326, ISSN: 0031-8965
- Trinkler, L.; Christensen, P.; Larsen, N.A. & Berzina, B. (1998). Thermoluminescence properties of AlN ceramics. *Rad. Meas.*, Vol. 29, (May 1998), No. 3-4, ISSN: 1350-4487
- Trinkler, L. ; Bos, A.J.J. ; Winkelman, A.J.M. ; Christensen, P. ; Agersnap Larsen, N. & Berzina, B. (1999). Thermally and optically stimulated luminescence of AlN-Y₂O₃ ceramics after ionising irradiation. *Radiation Protection Dosimetry*, Vol. 84, Nos. 1-4, (August 1999), pp. 207-210, ISSN: 0144-8420
- Trinkler, L.; Botter-Jensen, L.; Christensen, P. & Berzina, B. (2000). Studies of aluminium nitride ceramics for application in UV dosimetry. *Radiation Protection Dosimetry*, Vol. 92, No. 4, (March 2000), pp. 299-306, ISSN: 0144-8420
- Trinkler, L. & Berzina, B. (2001a). Radiation induced recombination processes in AlN ceramics. *J. Phys. : Condens. Matter*, Vol. 13, (September 2001), pp. 8931-8938 ; ISSN: 0953-8984
- Trinkler, L ; Botter-Jensen, L. ; Christensen, P. & Berzina, B. (2001b). Stimulated luminescence of AlN ceramics induced by ultraviolet radiation. *Rad. Meas.*, Vol. 33, No. 5, (October 2001), pp.731-735, ISSN: 1350-4487
- Trinkler, L. ; Botter-Jensen, L. & Berzina, B. (2002). Aluminium nitride ceramics: a potential dosimeter material. *Radiation Protection Dosimetry*, Vol. 100, Nos. 1-4, (April 2002), pp. 313-316, ISSN: 0144-8420
- Trinkler, L. ; Berzina, B. & Benadbesselam, M. (2003). Use of AlN ceramics in ultraviolet radiation dosimetry. *Proceedings of SPIE* Vol. 5123, (November 2003), pp. 49-54, ISSN: 0277-786X
- Trinkler, L. ; Berzina, B. ; Shi, S. C. ; Chen, L.-Ch. ; Benabdesselam, M. & Iacconi, P. (2005). UV light induced luminescence processes in AlN nanotips and ceramics. *phys. stat. sol. (c)*, Vol. 2, No. 1, (January 2005), pp. 334-338, ISSN: 1862-6351

- Trinkler, L.; Berzina, B.; Auzina, A.; Benabdesselam, M. & Iacconi, P. (2007a). UV light energy storage and thermoluminescence in AlN ceramics. *phys. stat. sol. (c)*, Vol. 4, No. 3, (March 2007), pp. 1032-1035, ISSN: 1862-6351
- Trinkler, L.; Berzina, B.; Auzina, A.; Benabdesselam, M. & Iacconi, P. (2007b). Use of aluminum nitride for UV radiation dosimetry. *Nuclear Instr. And Methods in Physics Research A*, Vol. 580, (May 2007), pp. 354-357, ISSN: 0168-9002
- Youngman, R.A. & Harris, J.H. (1990). Luminescence studies of oxygen-related defects in aluminum nitride. *J. Am. Ceram. Soc.*, Vol. 73, No. 11, (November 1990), ISSN: 0002-7820



Advances in Ceramics - Characterization, Raw Materials, Processing, Properties, Degradation and Healing

Edited by Prof. Costas Sikalidis

ISBN 978-953-307-504-4

Hard cover, 370 pages

Publisher InTech

Published online 01, August, 2011

Published in print edition August, 2011

The current book consists of eighteen chapters divided into three sections. Section I includes nine topics in characterization techniques and evaluation of advanced ceramics dealing with newly developed photothermal, ultrasonic and ion sputtering techniques, the neutron irradiation and the properties of ceramics, the existence of a polytypic multi-structured boron carbide, the oxygen isotope exchange between gases and nanoscale oxides and the evaluation of perovskite structures ceramics for sensors and ultrasonic applications. Section II includes six topics in raw materials, processes and mechanical and other properties of conventional and advanced ceramic materials, dealing with the evaluation of local raw materials and various types and forms of wastes for ceramics production, the effect of production parameters on ceramic properties, the evaluation of dental ceramics through application parameters and the reinforcement of ceramics by fibers. Section III, includes three topics in degradation, aging and healing of ceramic materials, dealing with the effect of granite waste addition on artificial and natural degradation bricks, the effect of aging, micro-voids, and self-healing on mechanical properties of glass ceramics and the crack-healing ability of structural ceramics.

How to reference

In order to correctly reference this scholarly work, feel free to copy and paste the following:

Laima Trinkler and Baiba Berzina (2011). Luminescence Properties of AlN Ceramics and Its Potential Application for Solid State Dosimetry, *Advances in Ceramics - Characterization, Raw Materials, Processing, Properties, Degradation and Healing*, Prof. Costas Sikalidis (Ed.), ISBN: 978-953-307-504-4, InTech, Available from: <http://www.intechopen.com/books/advances-in-ceramics-characterization-raw-materials-processing-properties-degradation-and-healing/luminescence-properties-of-aln-ceramics-and-its-potential-application-for-solid-state-dosimetry>

INTECH
open science | open minds

InTech Europe

University Campus STeP Ri
Slavka Krautzeka 83/A
51000 Rijeka, Croatia
Phone: +385 (51) 770 447
Fax: +385 (51) 686 166
www.intechopen.com

InTech China

Unit 405, Office Block, Hotel Equatorial Shanghai
No.65, Yan An Road (West), Shanghai, 200040, China
中国上海市延安西路65号上海国际贵都大饭店办公楼405单元
Phone: +86-21-62489820
Fax: +86-21-62489821

© 2011 The Author(s). Licensee IntechOpen. This chapter is distributed under the terms of the [Creative Commons Attribution-NonCommercial-ShareAlike-3.0 License](https://creativecommons.org/licenses/by-nc-sa/3.0/), which permits use, distribution and reproduction for non-commercial purposes, provided the original is properly cited and derivative works building on this content are distributed under the same license.

IntechOpen

IntechOpen